Quantitative proteomic analysis of HIV-1 infected CD4+ T cells reveals an early host response in important biological pathways: Protein synthesis, cell proliferation, and T-cell activation

Arti T. Navare [a], Pavel Sova [a], David E. Purdy [a], Jeffrey M. Weiss [a], Alejandro Wolf-Yadlin [c], Marcus J. Korth [a], Stewart T. Chang [a], Sean C. Proll [a], Tahmina A. Jahan [d], Alexei L. Krasnoselsky [a], Robert E. Palermo [a], Michael G. Katze [a,b,*]

[a] Department of Microbiology, University of Washington, Seattle, WA, USA
[b] Washington National Primate Research Center, University of Washington, Seattle, WA, USA
[c] Department of Genome Sciences, University of Washington, Seattle, WA, USA
[d] Proteomics Resource, UW Medicine at South Lake Union, Seattle, WA, USA

ARTICLE INFO

ABSTRACT

Human immunodeficiency virus (HIV-1) depends upon host-encoded proteins to facilitate its replication while at the same time inhibiting critical components of innate and/or intrinsic immune response pathways. To characterize the host cell response on protein levels in CD4+ lymphoblastoid SUP-T1 cells after infection with HIV-1 strain LAI, we used mass spectrometry (MS)-based global quantitation with iTRAQ (isobaric tag for relative and absolute quantification). We found 266, 60 and 22 proteins differentially expressed (DE) (P-value ≤ 0.05) at 4, 8, and 20 hours post-infection (hpi), respectively, compared to time-matched mock-infected samples. The majority of changes in protein abundance occurred at an early stage of infection well before the *de novo* production of viral proteins. Functional analyses of these DE proteins showed enrichment in several biological pathways including protein synthesis, cell proliferation, and T-cell activation. Importantly, these early changes before the time of robust viral production have not been described before.

Published by Elsevier Inc.

Introduction

During the 30-year history of Acquired Immunodeficiency Syndrome (AIDS), more than 60 million people have been infected with its causative agent, HIV-1, and more than 25 million people have died (UNAIDS, 2009). While treatment options exist for AIDS, it still remains a significant challenge worldwide with an estimated 2.6 million people newly infected every year and 1.8 million people succumbing to the disease (UNAIDS, 2009). Therefore, research in HIV biology is of critical importance for development of new antiviral treatment modalities.

Among the hallmarks of HIV-1 infection is disruption of the adaptive immune system caused by gradual depletion of CD4+ T cells (Gruters et al., 1990) leading to a slow decline in immune functions, with eventual failure to control normally tolerated pathogens. Like all viruses, HIV-1 depends upon the host cellular machinery for its survival and replication, orchestrated by

complex interactions between host and viral biomolecules (Bushman et al., 2009; Jager et al., 2012; MacPherson et al., 2010; Pinney et al., 2009). These interactions modulate host cell processes to facilitate expression of viral structural proteins, assembly of progeny virions and their release. Moreover, the virus has evolved ways to inhibit the antiviral host cell response by interacting with critical components of innate and/or intrinsic immune response pathways (Malim and Emerman, 2008). While the transcriptional processes affected by viral infection have been extensively studied, the knowledge of protein level changes is relatively limited. Recent advances in more sensitive and high throughput mass spectrometry(MS)-based methods, and bioinformatics tools has allowed studying the complex and dynamic range of the cellular proteome (Aebersold and Mann, 2003; Borchers and Tomer, 1999; Han, Aslanian, and Yates, 2008; Melendez et al., 2011). Quantitative MS-based approaches have been recently implemented to study changes in host protein abundance in T-cells upon HIV-infection (Chan et al., 2007; Chan et al., 2009; Ringrose et al., 2008) or in the presence of viral protein expressed from a plasmid (Coiras et al., 2006). These previous studies showed that the majority of host protein abundance changes occurred at the time when intracellular viral

production reached its maximum while the levels of only a few proteins have been shown to change early after HIV infection. It is possible that potentially important but subtle changes in protein levels as early as 4 hpi were not measurable due to lower specificity, sensitivity, and accuracy of the previously used fluorescence two-dimensional differential in-gel electrophoresis (2D-DIGE) (Ringrose et al., 2008) and proteolytic ^{18}O labeling quantitation methods (Chan et al., 2007).

Our study is an effort to fill this gap in knowledge of very early changes in host proteins after HIV infection. We used the isobaric tag for relative and absolute quantitation (iTRAQ) method suitable for comparative analysis of complex sample mixtures with high precision (Ross et al., 2004; Wolf-Yadlin et al., 2007; Wu et al., 2006) to measure global protein abundance in the CD4+ T cell line SUP-T1, at 4, 8, and 20 hours post infection (hpi) with HIV-1 (strain LAI). Our new data revealed temporal changes in host proteome, most prominently in the ribosomal proteins and translational machinery starting as early as 4 hpi, suggesting that HIV might disrupt cellular functions of the infected T-cell even before the time of peak intracellular viral protein and virion production.

Results and discussion

Here we describe changes in the global proteome of the T lymphocyte cell line CD4+ SUP-T1 during the course of HIV-1 infection. We used an MOI of 2.5, which resulted in close to 100% infection rate and collected samples in triplicate at 4, 8 and 20 hpi for both infected and time-matched mock infection. *De novo* viral RNA expression in this system was not detected by real-time PCR until 12 hpi, after which there was a rapid increase in expression between 12 and 24 hpi (Fig. 2a). This trend closely matched the detection of the HIV Gag protein (Fig. 2b). Gag was only detected at close to background levels at 4 and 8 hpi, followed by a significant increase by 20 hpi. Therefore, we established that the early 4 and 8 hpi time points are associated with minimal *de novo* production of viral proteins.

Distribution of subcellular locations and functions of the detected T-cell proteome

We detected 2847 proteins, which are distributed among main subcellular compartments as shown in Suppl. Fig. S4. Public annotations indicate that 51% of the detected proteins are
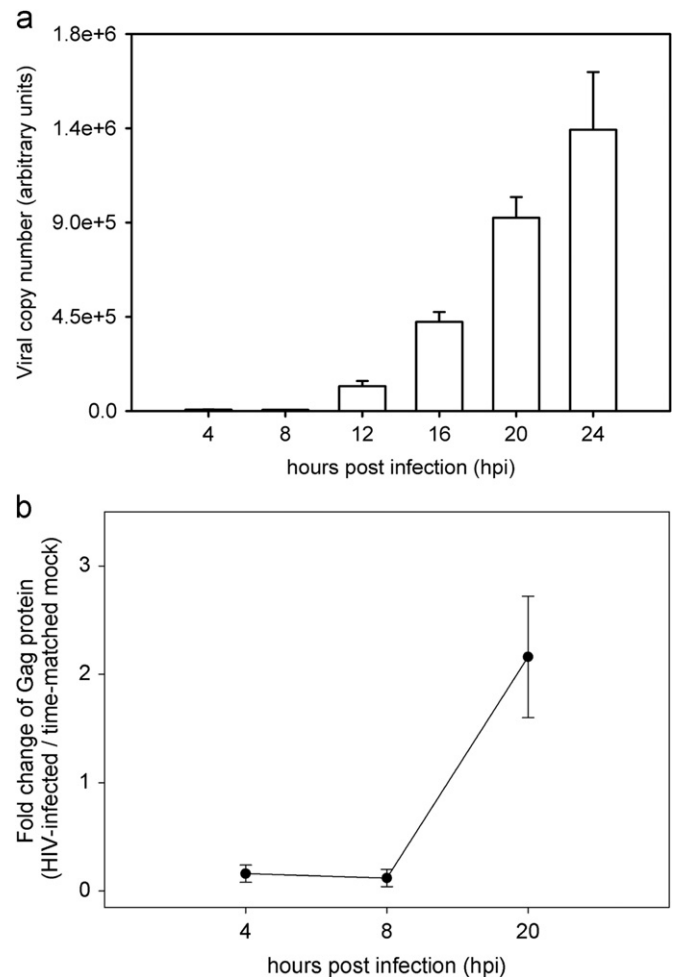
Fig. 2. (a) Real time PCR was used to determine relative viral RNA copy number (y-axis) in supernatants of infected SUP-T1 cells at different times post infection (x-axis). (b) Abundance change of HIV protein Gag over the course of infection, as determined by iTRAQ quantitation. The fold change ratio of the Gag protein (y-axis) is expressed relative to the intensity of the corresponding iTRAQ reporter ion for the mock-infected sample at 4, 8 and 20 hpi (x-axis). There is no detectable Gag protein in mock-infected samples and the ratio represents the fold-change over the background intensity. The error bars represent the standard deviation between three independent biological replicates.

nuclear, while cytosolic proteins accounted only for 5% of the total detected proteome. The remaining 45% of proteins were the constituents of mitochondrion, cytoskeleton, and plasma membrane. Such overrepresentation of nuclear proteins is expected for lymphocytes such as SUP-T1 that have small amounts of cytosol.

Out of all detected peptides 22% corresponded to the highly abundant ribosomal and other cellular housekeeping proteins (5% and 17%, respectively), while the remaining 78% corresponded to proteins of relatively lower abundance. The ability to detect the latter proteins was due to the sample fractionation steps prior the MS analysis steps (see Methods), as well as the result of fast scan rate (~1 Hz) of the mass spectrometer, which increased the chance of low abundant peptide ions to get identified in the presence of the peptide ions of highly abundant proteins.

Temporal quantitative changes in host proteome after HIV infection

We have confidently quantified by MS-based iTRAQ analysis 1448 out of 2847 detected cellular proteins (with 2 or more unique peptides). A t-test on protein level (see Methods) was performed for each time point individually to derive proteins
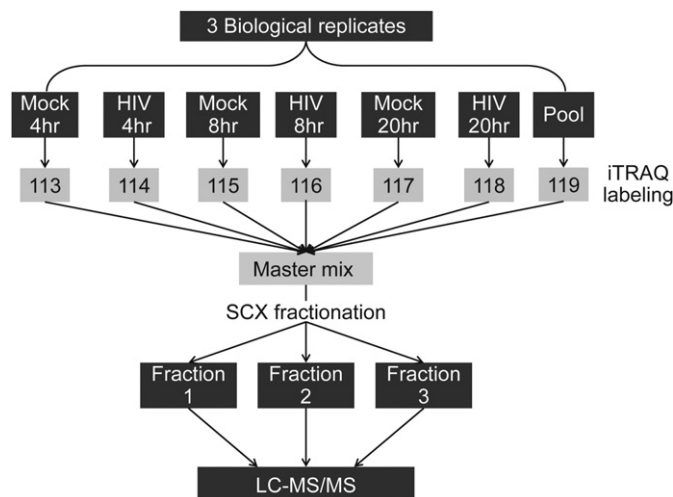

Fig. 1. iTRAQ sample preparation scheme. Samples, including the pools from each single biological replicate were labeled using iTRAQ labels 113–119. Labeled samples were mixed prior fractionation using Strong Cation Exchange (SCX) resin.

differentially expressed between HIV-infected and mock-infected SupT1 cells (results are shown in Table 1). We further filtered statistically significant proteins with the adjusted *P-value* < 0.05 by selecting a fold-change (FC) cutoff of ± 1.4 (infected/mock). This FC cutoff was selected based on the estimation of variation in protein abundance ratios in mock-infected samples at 4 and 8 hpi based on the assumption that no biologically significant changes are expected for the mock samples within this 4 h window (Fig. 3). As shown in the histogram in Fig. 3, 7.4% of such ratios showed FC of 1.4 or more and 2.6% of ratio showed FC of 1.4 or less. Therefore, an overall expectation of finding fold changes ± 1.4 due to technical variation between cell culture replicates is ~10%. We used this FC cutoff and applied a t-test filter ($P \leq 0.05$, B–H adjusted) to derive 348 statistically significant proteins, which showed differential abundance in at least one time point (Table 1). Surprisingly, most of the detected DE proteins (266/348) exhibited changes at 4 hpi as compared to the 60 DE proteins at 8 hpi, and 22 DE proteins at 20 hpi. It is unlikely that the low number of statistically significant proteins observed 20 hpi is due to higher variability between triplicates or in the ratios for that time point as the histogram of all observed protein ratios does not reflect an increase in variability (Suppl. Fig. S3). The overlap of the 348 DE

proteins ($P \leq 0.05$, FC ≥ 1.4) at the three time points is shown in the Venn diagram in Fig. 4a. Only 25 DE proteins are shared between the early time points (4 and 8 hpi), while only one protein (UTP14A, U3 small nucleolar RNA-associated protein 14) overlapped between 8 and 20 hpi DE lists. The small overlap between the early time points vs. the late time point suggests that completely different sets of host proteins or processes were perturbed in these times.

A global view of the protein abundance changes of the 348 DE proteins is shown in Fig. 4b. The directionality of abundance changes for 22 of the 25 overlapping DE proteins between 4 and 8 hpi remained consistent at these time points (4b). It is noteworthy that we observed down regulation of HIV-1 dependency factor Tat specific factor 1 (HTATSF1) implicated by some investigators in regulation of Tat transactivation in viral RNA transcription (Brass et al., 2008; Zhou and Sharp, 1996) and in general regulation of cellular mRNA transcription and splicing (Miller et al., 2011). Two additional commonly changed (upregulated) proteins in both early time points, namely GPI and SLC3A2 have been shown to interact with HIV-1 proteins, suggesting that the levels of host interactors are possibly manipulated early on in the course of HIV infection.

We further investigated what key cellular functions might be associated with the protein abundance changes of 348 DE proteins. We used IPA to perform functional analysis using 2847 detected proteins as a reference list. The results are summarized

Table 1
Differentially expressed (DE) cellular proteins in HIV-infected CD4+ SUP-T1 cells.

	No. of DE[a] proteins at		
	4 hpi	8 hpi	20 hpi
Up-regulated proteins			
FC[b] $\geq$ 1.4	117	26	4
FC $\geq$ 2	18	2	0
Down-regulated proteins			
FC $\geq$ 1.4	149	34	18
FC $\geq$ 2	55	7	7

[a] Differentially expressed (DE) proteins are the proteins that showed abundances changes in the HIV-infected cells as compared to their time-matched mocks with a nominal (*P-value* < 0.05).
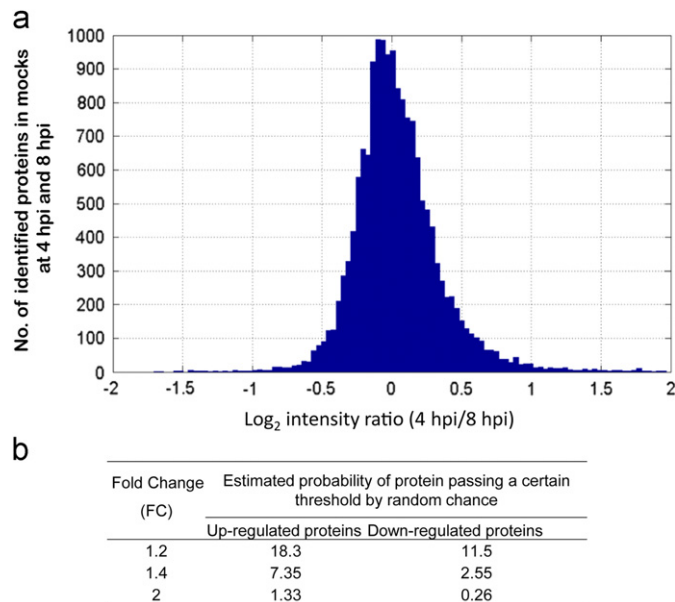[b] FC, fold change.

Fig. 3. (a) Histogram of number of identified proteins and their log$_2$ intensity ratio at 4 hpi/8 hpi. The histogram was used to determine the number of DE proteins passing fold change thresholds of 1.2, 1.4, and 2.0 by random chance. (b) Table of estimated probabilities of a DE protein at different FC thresholds.
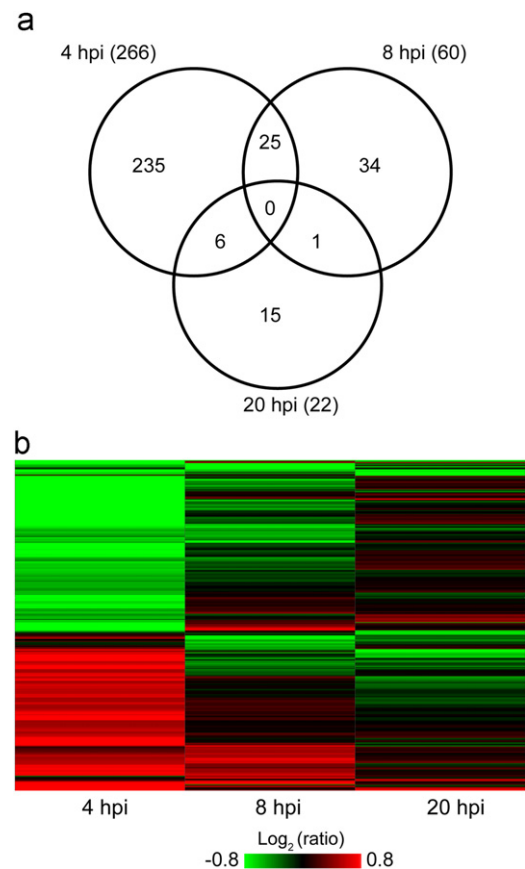

Fig. 4. (a) Overlap of the 266 DE proteins at 4 hpi, 60 DE proteins at 8 hpi, and 22 DE proteins at 20 hpi (348 total DE proteins) with FC $\geq$ 1.4, and *P-value* $\leq$ 0.05 in at least one time point is shown in the Venn diagram. (b) Heatmap of the 348 cumulatively DE proteins in at least one time point is plotted by hierarchical clustering of the DE proteins based on the log$_2$ intensity ratios of HIV-infected to time-matched mock-infected samples at 4, 8, and 20 hpi. The directionality of protein abundance change is denoted by red (upregulated, FC $\geq$ 1.4), green (downregulated, FC $\leq$ 1.4) and black (unchanged) colored bars.
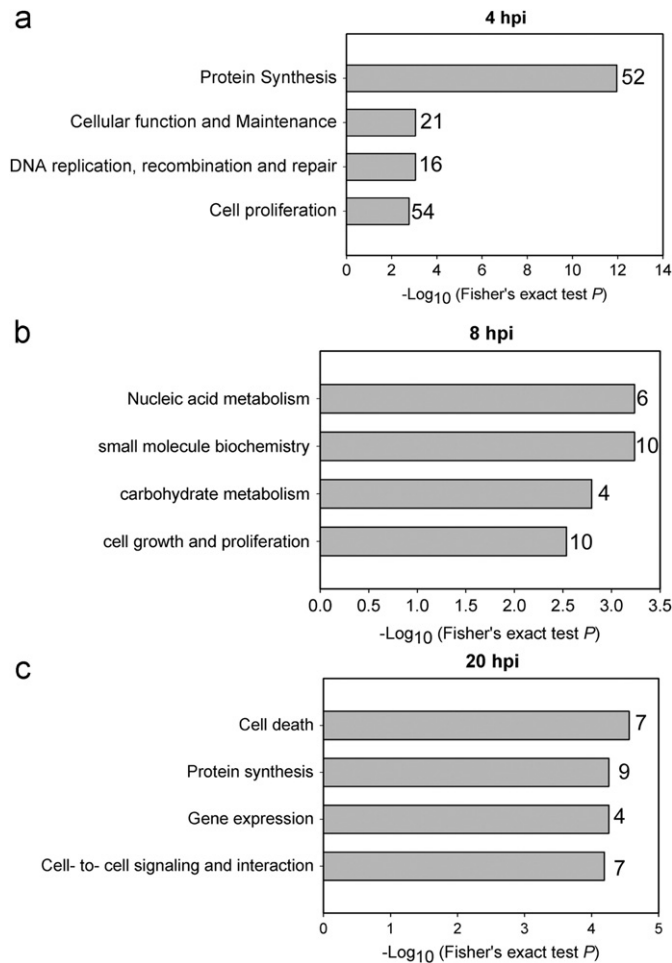
Fig. 5. Top biological functions associated with DE proteins as identified by IPA at (a) 4 hpi, (b) 8 hpi, and (c) 20 hpi. The enrichment score ($-\log_{10}$ transformed) associated with each category are shown (horizontal axis) along with the number of DE proteins on right. The DE proteins had a fold change (FC) of ≥ 1.4 and t-test associated $P\text{-value} < 0.05$ in at least one time point.

in Fig. 5. Different cellular functions were enriched at three time points and the enriched functional categories at 4 hpi, namely, protein synthesis, cell proliferation, DNA recombination, repair and maintenance were associated with the most DE proteins, in contrast to the categories enriched at 8 and 20 hpi. Taken together, this suggests that the infected T cell shows sign of brief cell protein biogenesis and proliferation and maintenance which then subsides with the progression of infection.

Proteins associated with protein synthesis increased in abundance at 4 hpi

Four hours after infection marks a point in HIV-1 life cycle when internalized virions have undergone uncoating, reverse transcription of genomic RNA, translocation of preintegration complexes to the nucleus and integration of viral cDNA in host cell genome. Attendant to these processes is the cellular response to binding and internalization of virus particles as well as changes triggered by interactions of the internalized virus proteins with their cellular binding partners. Consistent with this notion, we found protein synthesis as the most enriched category (*P*-value 1.12E-12) with 52 DE proteins at 4 hpi, while at 20 hpi 9 DE proteins were associated with this category (*P*-value 5.55E-5) (Fig. 5c). We found only 4 DE proteins associated with protein synthesis (ETF1, SLC7A1, RPS5, TFRC) commonly changing at 4 and 20 hpi (Suppl. Table S2). Notably, eukaryotic translation

termination factor 1 (ETF1) was strongly downregulated early after infection, and remained still significantly downregulated at the 20 hpi time point, unlike most other proteins involved in protein synthesis (discussed below). These proteins are first upregulated at 4 hpi, which is followed by downregulation or no change at late time point. ETF1 participates in protein synthesis as a polypeptide chain release factor directing termination of mRNA translation from the stop codons, and also in nonsense-mediated decay of prematurely terminated mRNAs. Membrane proteins solute carrier family 7 (cationic amino acid transporter), member 1 (SLC7A1) and transferrin receptor (TFRC) were noted as significantly downregulated in both early and late time points (SLC7A1) or up- and downregulated, respectively. Decrease of TFRC (CD71) abundance during HIV-1 infection has been described previously (Madrid et al., 2005) and associated with nef-induced alteration of trafficking of surface proteins involved in adaptive immunity and HIV-1.

About 69% of the proteins (36 out of 52) involved in protein translation at 4 hpi were ribosomal, eukaryotic translation elongation, or initiation factors that showed increased abundances in the virus-infected cells at 4 hpi (Suppl. Table S2). As summarized in Fig. 6a, differential protein abundance was found for the components of both ribosomal subunits. With few exceptions, these same proteins showed a decrease or no change in abundance at 8 and 20 hpi (Fig. 6b and c; for complete list of proteins,
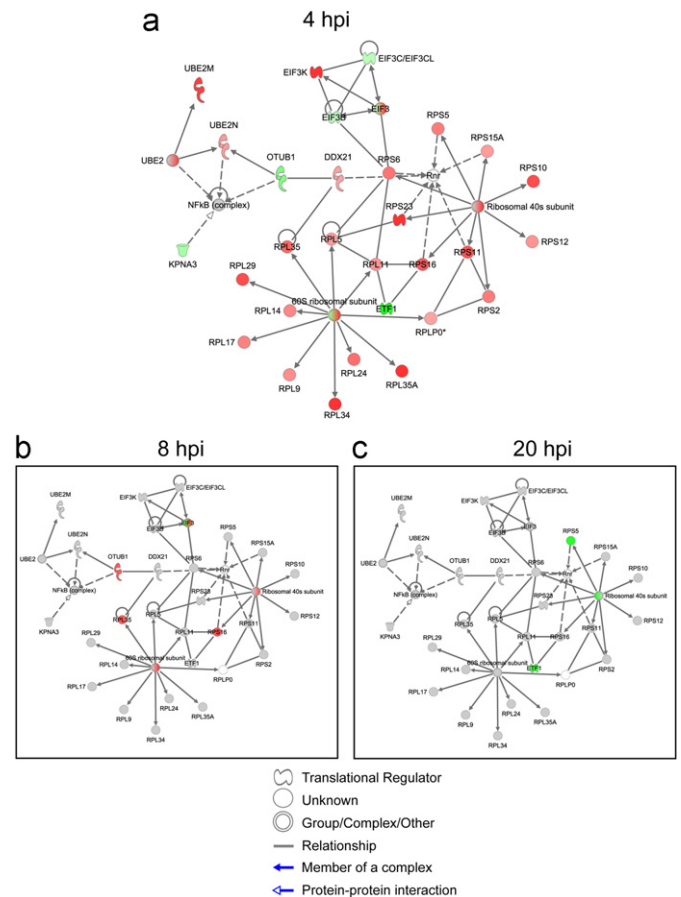

Fig. 6. Network derived from functional analysis of the DE proteins in IPA showing connections among DE protein synthesis-related proteins (a) at 4 hpi. The majority of members of this network belong to ribosome assembly and translation factors. These proteins were upregulated (in red), with few exceptions such as EIF3C which was downregulated (in green). Time-course changes in protein abundance of these proteins at 8 hpi (b) and 20 hpi (c). for the network described in (a). (For interpretation of the references to color in this figure legend, the reader is referred to the web version of this article.)
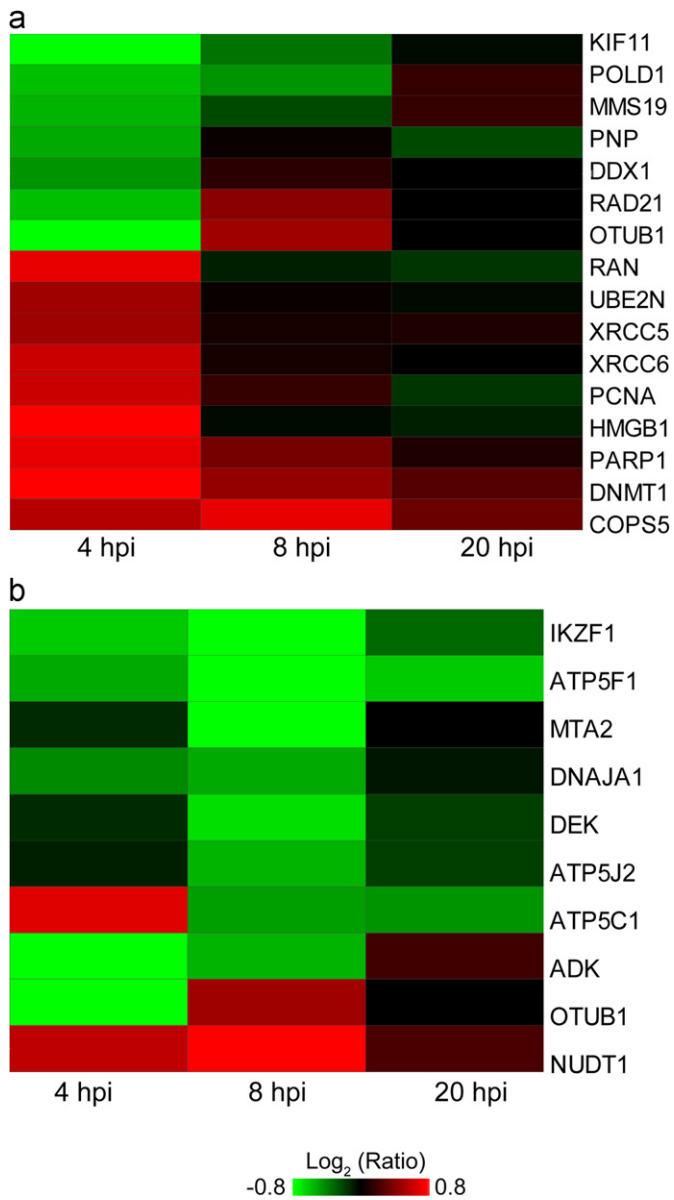
Fig. 7. Heatmap of (a) 16 DE proteins enriched in DNA repair and recombination functional category at 4 hpi and (b) 10 DE proteins associated with this category at 8 hpi. A single protein OTUB1 involved in DNA double-strand breakup was found DE at both time points (4 and 8 hpi). However this protein showed different directionality in abundance level changes at these time points. The directionality of protein abundance change is denoted by red (upregulated, FC $\geq$ 1.4), green (downregulated, FC $\leq$ 1.4) and black (unchanged) colored bars. (For interpretation of the references to color in this figure legend, the reader is referred to the web version of this article.)

see supplemental Table S2). With the exception of 4 hpi, protein synthesis was down-regulated over the course of the infection as one might expect from previous reports (Chan et al., 2009). However, it is very surprising that protein synthesis was elevated at 4 hpi, as judged by DE proteins. Ribosomal proteins, among many other housekeeping (HK) proteins, are commonly regarded as constitutively expressed in eukaryotic cells, raising a concern that the observed effect at 4 hpi was a possible artifact introduced by normalization. To eliminate this possibility, we examined the expression levels of the other known HK proteins in our dataset. We used a list of 566 human HK genes (Eisenberg and Levanon, 2003) (http://www.compugen.co.il/supp_info/Housekeeping_genes.html), that includes genes for 40 ribosomal proteins and 7 translation and elongation factors. Excluding the ribosomal and eukaryotic translation

initiation and elongation proteins, 220 HK proteins were detected in our dataset. The fold change ratios of these proteins (HIV: Mock) were calculated for 4 hpi data. We found that 97% of HK proteins (214/220) did not show significant change in abundance (FC $\geq$ 1.4) (Suppl. Fig. S5). This analysis suggests that the observed increase in abundance of the ribosomal and translation related proteins is not a methodological artifact, as we would anticipate this impacting all the housekeeping proteins.

Such abundance changes in the protein synthesis machinery have not been previously reported in HIV-1-infected CD+T cells, especially at such an early time point. Infection of T cells by HIV-1 has been previously associated with reduced transcript levels for several elongation initiation factors, ribonucleoprotein complex/ ribosome assembly and protein synthesis at later (24 hpi) time points (van't Wout et al., 2003). Chan et al. described similar changes in the ribosomal proteins of HIV-1 infected primary T-cells at 8 hpi, albeit with far fewer identified proteins (Chan et al., 2009).

The upregulation of ribosomal proteins at 4 hpi, may indicate post-transcriptional regulation. mRNAs encoding ribosomal proteins, contain 5'UTR terminal Oligopyrimidine (TOP) tracts that regulate their translational activity (Levy et al., 1991) through interaction with a number of RNA-binding proteins, including RPS6 (Hagner et al., 2011). Up-regulation of RPS6 is associated with protein synthesis and cell proliferation, during which this ribosomal protein is activated by phosphorylation by 40S ribosomal protein S6 kinase (p70-S6K) (Meyuhas, 2008). p70-S6K is in turn activated as a consequence of a variety of signal transduction cascades such as Akt2 and mTOR but it has been also observed that Env gp41can activate the p70-S6K subunit RBS6KB1(Barcova et al., 1999), although this latter data was not explicitly derive from an actual infection model. It is therefore conceivable that HIV-1 elicits early proliferative response target cells, with many components driven by post-transcriptional regulation.

We observed enrichment of protein synthesis functional category also at 20 hpi, however it pertained to a different set of 9 DE proteins, and except for a protein product of gene RSL1D1 (ribosomal protein L1 domain), abundances of these proteins were decreased (Suppl. Fig. S6). Interestingly, RSL1D1 protein did not change significantly at early hours (4 and 8 hpi) of infection but showed 1.6- fold increase at 20 hpi. This protein has been showed to be involved in protein localization of nucleolar proteins (Meng et al., 2006) as well as it has been identified in siRNA screen as a dependency factors for HIV-1 infection (Brass et al., 2008).

Changes in cell proliferation and DNA repair, recombination and maintenance

Increased abundance of proteins involved in ribosome biogenesis and in protein synthesis typically reflects a cellular state with higher biosynthetic demand, such as in proliferating cells (Montanaro et al., 2008). As described above, cell proliferation is among the top functional categories (*P-value* 7.43E-3) at 4 hpi with 54 DE proteins (Suppl. Table S3), of which a slight majority was upregulated (35 vs. 24 downregulated; with a few exceptions, these proteins did not show significant changes at 8 and 20 hpi). While one of the hallmarks of HIV-1 infection is cell death by apoptosis, it is possible that the initial response to the virus binding to the cell surface is proliferative. The crosslinking of the HIV-1 envelope protein and CD4 and CXCR4 virus receptor and co-receptor may trigger some aspect of TCR (T cell receptor) signaling, providing a proliferative signal to the recipient T cells that are not actively proliferating under physiological conditions (Kornfeld et al., 1988; Misse et al., 1999). It is therefore conceivable that interaction of the viral envelope protein with CD4 receptor primes CD4+ SUP-T1 cells for a proliferative response

that may activate biosynthesis of the translation apparatus, however, this response is brief and ultimately overshadowed by viral cytotoxicity leading to apoptosis and necrosis.

Several proteins involved in DNA repair and recombination process changed in abundance at 4 hpi (16 DE proteins, Fig. 7a) and 8 hpi (10 DE proteins, Fig. 7b), suggesting that this category was highly affected early during the infection (Suppl. Table S4). The two sets of DE proteins at 4 and 8 hpi had a single protein in common, ubiquitin thioesterase (OTUB1). This deubiquitinating enzyme suppresses RNF168-dependent ubiquitination of the DNA double-strand breaks by binding ubiquitin-conjugating enzyme E2N (UBE2N) (Nakada et al., 2010). We identified OTUB1 and UBE2N changing in opposite directions at 4 hpi, where OTUB1 was significantly downregulated and UBE2N was upregulated. Functionally, this would allow more chromatin ubiquitination at double-stranded breaks, leading to more efficient localization of the genome repair machinery, suggesting there is initial attempt of the infected cells to control the DNA damage due to infection. However at 8 hpi, the deubiquitinating enzyme OTUB1 was upregulated (1.4-fold), while the abundance level of UBE2N returned to the level observed in mock-infected cells, and by 20 hpi, both proteins were unchanged compared to their levels in the time-matched mocks. As a consequence, the initial DNA damage response has declined, as the levels of UBE2N and other proteins involved in DNA repair and mitosis checkpoint activation returned to those observed in time-matched mocks (Fig. 7).

T-cell functions affected throughout the course of the infection

At the late time point (20 hpi) we found that almost 32% of the 22 DE proteins were enriched for activation-induced cell death of T lymphocytes (P-value 2.75E-5) (Fig. 5c). Proteins involved in T-cell activation and cell-mediated immune response (LCK, SPN, RAC2, PARP1, HSPD1, HMGB1) were altered at 20 hpi, and some at 4 hpi (Suppl. Table S5). T-cell activation-related proteins LCK (Lymphocyte specific protein kinase), SPN (sialophorin), and RAC2 (ras-related C3 botulinum toxin substrate 2) were down-regulated at 20 hpi. Down-regulation of LCK on protein level is consistent with the previously observed transcriptional level changes of this protein (Chang et al., 2011). SPN protein which has been reported to participate in T-cell migration (Cannon et al., 2011) remained down-regulated at early and later time points, while RAC2, which is implicated in T-cell activation (Ramaswamy et al., 2007) and proliferative response (Bustelo, 2002) was initially up-regulated but then decreased at 20 hpi. Heat shock protein 60 (HSPD1) has been shown to play a role in the chemotactic migration of T cells in blood (Zanin-Zhorov et al., 2003) as well as in binding with HIV gp41 membrane protein (Speth et al., 1999). The later interaction of HSPD1 with the HIV membrane protein is more relevant in our study, where the increased levels of this protein at 4 hpi potentially help the entry of the virus. HMGB1, a nuclear protein which is known to play a significant role in DNA architecture(Bonaldi et al., 2003) has also been implicated in cell signaling(Wang et al., 1999). Overall, the differential expression of proteins related to T-cell activation upon HIV infection indicates that HIV-1 infection elicited protein abundance changes that may lead to suppression of T-cell immune function during the entire course of infection, and not just at the later time point.

Differentially regulated host proteins with known viral–host protein interactions

We cross-examined our list of 348 DE proteins with those known to interact with HIV proteins by searching against previously published HIV-human protein–protein interactions databases,

such as the recently developed 'Human Immunodeficiency Virus Type 1 (HIV-1), 'Human Protein Interaction database' (HHPID) at NCBI, (Fu et al., 2009; Pinney et al., 2009; Ptak et al., 2008) and the recently published database by Jager et al. (2012). HHPID contained1439 unique proteins and over 2500 unique HIV-human protein–protein interactions (PPIs), while Jäger's database comprised of 242 unique proteins with 497 interactions. We found our DE set of proteins enriched in HIV interactors with 65 (P-value ≤ 0.015) and 26 (P-value ≤ 0.083) matched with HHPID and Jäger's databases, respectively, with 4 DE proteins, namely KARS, RANBP1, PSMB6, VPRBP, overlapping between the two sets (Table 2; marked by asterisk). Of these 4 DE proteins, levels of KARS were down regulated from 8 hpi through 20 hpi, while the remaining three proteins were only changed at 4 hpi. Notably, we found that the abundance of karyopherin alpha 3 (importin alpha 4) transiently decreased at 4 hpi. The role of this protein in the nuclear import of HIV pre-integration complex via its interaction with incoming virion matrix protein has been reported (Bukrinsky and Haffar, 1998), and the reduced abundance would be expected to mitigate the extent of incorporation of viral genome. Transferrin receptor CD71 showed a transient increase at 4 hpi, HIV Nef protein (also present in viral particles) disrupts the endosomal trafficking of CD71 to enhance Nef-mediated viral infectivity (Madrid et al., 2005), and the disruption of CD71 degradation in the endosome could result in the increased abundance we observe. It is conceivable that interactions between the viral and cellular proteins modulate the quantity of the latter and thus promote viral replication in infected SUP-T1 cells.

Conclusions

In our study, we utilized a high-throughput quantitative proteomic analysis to identify changes in host cell protein abundance upon infection of CD4+ T cell line with HIV-1. We show here that virus infection triggers perturbations in host proteome at a very early stage of infection before de novo production of viral proteins. Among the most significantly affected cellular functions were protein synthesis (early upregulation), followed by down-regulation of proteins involved in cell proliferation, DNA repair and recombination, and maintenance of T cell immune function. These changes, some of which occur very early after infection, may suggest novel strategies by which the HIV-1 virus manipulates host cell machinery to its own advantage.

Materials and methods

Cells, virus, and infection

All procedures involving infectious HIV-1 were carried out in biosafety level (BSL) 2 lab with BSL 3 practices in accordance with the University of Washington biological safety guidelines (The University of Washington Environment Health and Safety, 2011). The T lymphoblastic leukemia cell line SUP-T1 was obtained from American Type Cell Culture collection (Manassas, VA; CRL-1942) and cultured in RPMI 1640 supplemented with penicillin (100 U/ml), streptomycin (100 μg/ml), GlutaMAX-I (Invitrogen, Carlsbad, CA) and 10% Fetal Bovine Serum (HyClone, Logan, UT). HIV LAI strain was obtained from NIH AIDS Research & Reference Reagent Program (Germantown, MD) and propagated in SUP-T1 cells. Viral titers were measured in U373-MAGI-CXCR4$_{CEM}$ cells obtained through the AIDS Research and Reference Reagent Program following a protocol by Emerman (Vodicka et al., 1997). Synchronous infections of SUP-T1 cells were carried out by suspending cells in a concentrated inoculum with a proportion of virus

Table 2
List of the T-cell DE proteins with known HIV-1 protein interactions was obtained by comparing the DE proteins from our dataset with the two published HIV-human protein-protein interaction databases (HHPID at NCBI and Jäger's database). Four DE proteins that were found in both databases are marked with an asterisk.

Cellular protein	Gene symbol	HIV protein	Log$_2$ (FC)
4 hpi			
Actin, beta	ACTB	Tat	0.66
X-ray repair complementing defective repair in Chinese hamster cells 6	XRCC6	Tat, Vif	0.63
X-ray repair complementing defective repair in Chinese hamster cells 5	XRCC5	Tat	0.50
RAN binding protein 1*	RANBP1	Vpu, Rev	0.73
Lactate dehydrogenase A	LDHA	Tat, Envelope gp41	0.53
Transferrin receptor (p90, CD71)	TFRC	Nef	0.53
moesin	MSN	Gag	0.50
Adapter-related protein complex 2, beta 1 subunit	AP2B1	Nef	−0.56
Proteasome subunit, beta type, 6*	PSMB6	GP140, GP120, Tat	−0.76
Karyopherin alpha 3 (importin alpha 4)	KPNA3	Matrix	−0.80
Vpr (HIV-1) binding protein*	VPRBP	Vpr	−1.10
Protein phosphatase 2, regulatory subunit B	PPP2R2A	Vpr	−1.23
8 hpi			
Importin 5	IPO5	Vpr	0.50
Glucose-6-phosphate isomerase	GPI	gp120	0.66
Solute carrier family 3	SLC3A2	gp160	0.76
Small nuclear ribonucleoprotein polypeptides B and B1	SNRPB	Tat	0.90
Lysyl-tRNA synthetase*	KARS	Matrix, Gag, Capsid	−0.47
HIV-1 Tat specific factor 1	HTATSF1	Tat	−0.47
20 hpi			
Vinculin	VCL	Nef	0.50
Caspase 3, apoptosis-related cysteine peptidase	CASP3	Vpr	−0.47
Lymphocyte-specific protein tyrosine kinase	LCK	Nef	−0.47
Transferrin receptor (p90, CD71)	TFRC	Nef	−1.06
Sialophorin	SPN	gp120	−1.73
Eukaryotic translation initiation factor 4 gamma	EIF4G1	Retropepsin	−0.56

corresponding to a multiplicity of infection (MOI) 2.5 for 1 h at 37 °C in an incubator with 5% CO$_2$ atmosphere. After this 1 h period of virus attachment and internalization, unattached virions were removed by washing the cells with an excess of fresh media and then plating the washed cells in fresh media at a density of 1×10^6 cells/mL. Infections were performed in triplicate. The infectious dose (MOI 2.5) was optimized to reach near 100% of cell infectivity. Infected cells were visualized by immuno-fluorescence assay with rabbit HIV-1$_{SF2}$ HIV p24 antiserum kindly provided by BioMolecular Technologies through the AIDS Research and Reference Reagent Program. HIV-1 mRNA relative abundance was measured using Taqman assay with a standard curve to ensure linearity of the assay (forward primer HXB2-Gag-F 5′-CAA GCA GCC ATG CAA ATG TT-3′, reverse primer SK431-B 5′-TGC TAT GTC ACT TCC CCT TGG TTC TCT-3′ and probe HXB2-gag 5′-FAM AAA GAG ACC ATC AAT GAG GAA GCT GCA GAA 3′-TAMRA).

Protein extraction, digestion and iTRAQ labeling

For each condition, 5 million SUP-T1 cells were collected by centrifugation at $1000 \times g$ for 5 min at 4 °C. Cell pellets were washed twice with cold Dulbeco's phosphate buffered saline then snap frozen and stored at −80 °C. Cell pellets were resuspended in 0.3 ml of urea buffer (8 M urea in 50 mM ammonium bicarbonate, pH 7.8) and denatured at room temperature for 1 h with agitation at 1000 rpm. The resulting suspensions were sonicated in a chilled water bath cup-horn (Qsonica, Newtown, CT) at 35% amplitude for 3 cycles (1 min pulse followed by 2 min on ice). Residual cell debris was removed by centrifugation at $16,000 \times g$ for 10 min at 4 °C, and the supernatant was collected. Total protein concentration was determined with Bio-Rad Protein Assay Dye Reagent using manufacturer's instructions (Bio-Rad, Hercules, CA).

All steps were performed at room temperature unless otherwise noted. Protein samples (245 µg) were reduced with 5 mM dithiothreitol for 1 h, then alkylated with 15 mM iodoacetamide for 30 min in the dark. Samples were diluted 8-fold with 50 mM ammonium bicarbonate (pH 7.8), then digested with Sequencing Grade Modified trypsin (Promega, Madison, WI) at a ratio of 1:50 (trypsin to protein) for 16 h at 37 °C. Peptides were desalted and concentrated using Discovery C18 SPE cartridges (Supelco, Bellefonte, PA) as per the manufacturer's recommendations then dried by vacuum centrifugation and stored at −80 °C.

We checked the efficiency of trypsinization of ribosomal proteins in HIV-infected and mock-infected protein extracts to rule out the possibility that the difference in the structural stability of the ribosomes in the HIV-infected cells might have affected the tryptic digestion, thus resulting in apparent differences in abundance. To investigate this possibility, we looked at the percentages of missed cleavages in ribosomal peptides. We did not find any bias toward any biological condition in our study. Therefore, we believe that difference in trypsinization as a potential source of variability did not contribute to the observed differences in abundance (see Results section).

iTRAQ labeling was carried out using iTRAQ Reagents 8-plex kit (AB Sciex, Foster City, CA) as recommended in the manufacturer's protocol. Fig. 1 shows a diagram of the peptide labeling scheme used in this study. Briefly, peptide pellets were resuspended in 3% acetonitrile and peptide concentration was determined by BCA assay (Pierce, Rockford, IL). For each sample, an equal peptide amount (43 µg) was aliquoted then dried by vacuum centrifugation. Peptide pellets were suspended in 0.5 M triethylammonium bicarbonate (pH 8.5) and labeled with 1 unit of the appropriate iTRAQ labeling reagents (113 through 119) for 2 h (Fig. 1). Additionally, we created a 'pool' sample by mixing ~7 µg of peptides from the 18 samples (3 HIV-infected and 3 time-matched mock at 4, 8, and 20 hpi) and labeled it with an iTRAQ label 119 (Suppl. Table S1) for use as a common reference

across individual iTRAQ multiplex experiments for subsequent normalization. Labeling reactions were then combined and the iTRAQ multiplex sample volume was reduced by vacuum centrifugation. Each iTRAQ multiplex experiment was fractionated off-line using Discovery Strong Cation Exchange (SCX) SPE cartridges (Supelco) as per manufacturer's recommendations with increasing concentrations (300, 400, 500, 600, and 1000 mM KCl, in 25% acetonitrile, 10 mM potassium phosphate monobasic, pH 3) of potassium chloride buffer. Fractions 300 mM and, 400 mM were combined into one fraction, and fractions 600 mM and 1 M were combined into a second fraction before proceeding with the desalting step. The third fraction with 500 mM KCl was not combined with the other fractions as it had the highest amount of peptide concentration, as determined by the BCA assay. Finally, the three KCl fractions were desalted using Discovery C18 SPE cartridges.

LC-MS/MS data acquisition

Online peptide separation followed by mass spectrometric analysis was performed on a 1D-nanoLC system (nanoAcquity UPLC system, Waters Corp.,Milford, MA, USA) coupled to a LTQ Orbitrap Velos mass spectrometer (Thermo Fisher Scientific, CA, USA), equipped with a high energy collision cell. Individual C-18 purified SCX fractions containing the iTRAQ labeled peptides were injected (4 μg/5 μL injection volume) in duplicates and captured onto a trap column packed with reverse phase beads (Symmetry®, C18, 5 μm particle size, 100 Å pore size, 5 cm packing length, 150 μm column i.d.). Peptide separation was achieved on an analytical nano-column (Symmetry®, C18, 5 μm particle size, 100 Å pore size, 15 cm packing length, 75 μm column i.d.) using a gradient from 3 to 80% of solvent B in A over 210 min (Solvent A: 100% water, 0.1% Formic acid (FA); Solvent B: 97% ACN/3% Water, 0.1% FA) at a flow rate of 200 nL/min. The effluent from the HPLC column was directly electrosprayed into the mass spectrometer.

The mass spectrometer was operated in data-dependent mode to automatically switch between MS and MS/MS acquisitions. The Top 10 method was used in the data-dependent mode where each full-scan MS (from m/z 300–2000) was acquired in the Orbitrap analyzer (resolution=60,000), followed by first high energy collision induced dissociation (HCD) MS/MS (from m/z 100–1700) and a subsequent low collision induced dissociation (CID) MS/MS scan of the top 10 most intense precursor ions with a charge states ≥ 2. The HCD MS/MS scans were acquired using the Orbitrap system (resolution=30,000) at normalized collision energy of 75% and the low-energy CID MS/MS scans were scanned in a low-pressure ion trap with a normalized collision energy of 35%. The ion selection threshold was set to 5000 counts for HCD, and 500 counts for CID scans. Precursor ion isolation width of 1.5 was used for the MS/MS scans and the maximum allowed ion accumulation times were set to 500 ms for full scans and 250 ms for HCD, and 25 ms for CID scans.

The standard mass spectrometer tune method settings were as follows: Spray voltage, 2.1 kV; no sheath and auxiliary gas flow; heated capillary temperature, 325 °C; Automatic Gain Control (AGC) enabled. All samples were analyzed by LC-MS/MS in duplicates, and an equimolar (500 fmol/μL) binary peptide standard mix of angiotensin I and neurotensin (Sigma-Aldrich, St. Louis, MO, USA) was used between the sample runs to check the run-to-run reproducibility of the LC-MS system.

Protein identification

Raw MS/MS data files were processed by Tagtraq (The University of Washington's Proteomic Resource Facility (UWPR), 2011), which merges HCD and CID MS/MS scans for each precursor ion and generates merged.mgf output files for every precursor ion detected by the mass spectrum. The merged.mgf files were imported into the 'Trans-Proteomic Pipeline' (TPP) (Deutsch et al., 2010) for protein identification using the X!Tandem search engine. The protein search was performed against a user defined database consisting of 35,284 human proteins (Original source: Uniprot_Human version, released on 2011-03-08), and 123 viral proteins containing protein sequences of HIV strains LAI, HXB2, BRU, and IIIB (obtained from GeneBank®, accessed in October 2010) (Benson et al., 2011). The following variable modifications were used: Oxidation of met (+15.994915 Da), carbamidomethylation of Cysteine (+57.021464 Da), and+304.2 Da at K due to iTRAQ 8-plex labeling of N-termini or lysine-side chains of tryptic peptides. All identified peptides (and corresponding proteins) passing with error rates $\leq 5\%$ and with corresponding Peptide-Prophet (Keller et al., 2002) probabilities ≥ 0.70 were retained. A total of 9749 unique peptides corresponding to 2847 unique proteins were identified across all the samples.

Protein quantitation by iTRAQ

Protein quantification based on the iTRAQ labels was performed with Libra software (Pedrioli et al., 2006) embedded in TPP. The intensity of label 119 from the pool sample was used to calculate the relative intensities of the other reporter ions (iTRAQ labels) in the 8-plex. We checked the between labels intensity variability by calculating correlation between two reporter ions of peptides identified in all three biological replicates. A tight overall correlation between each pair of iTRAQ ions was found ($R^2=0.99$) (e.g., see correlation plot for 113 and 114 ions, Suppl. Fig. S1). The Libra normalized $\log_{10}$ intensity ratios for each sample (each label) were normalized to the median of 0 under the assumption that the majority of proteins do not change in abundance. We checked the data quality of the iTRAQ quantitation datasets for 4, 8, and 20 hpi, by plotting scatter plots of intensities of iTRAQ labels for mock-infected samples as well as HIV-infected samples at 4 hpi vs 8 hpi (113 vs 115; 114 vs 116), 4 hpi vs 20 hpi (113 vs 117; 114 vs 118) and 8 hpi vs 20 hpi (115 vs 117; 116 vs 118) (Suppl. Fig. S2). A good overall correlation ($R^2=0.98-0.99$) between different conditions at different time points suggested that the iTRAQ data quality was comparable between the samples, and no bias was introduced by the normalization procedure. In order to maintain high quality data, all proteins with single peptide–peptide based identifications were excluded from further analysis.

Two-sample unequal variance t-test was performed to derive lists of differentially abundant proteins between infected and mock-infected samples at each time point. To correct for multiple hypothesis testing, we applied Benjamini–Hochberg (BH) P-value correction. The final list of differentially expressed (DE) proteins corresponded to the adjusted P-value ≤ 0.05. All computational data processing and statistical tests were performed using custom scripts in Perl and MATLAB, using the statistical toolbox (MathWorks, Inc., Natick, MA).

The accuracy of identification of 15 of the DE proteins that were identified by X!Tandem search engine with only 2 unique peptides were confirmed by manual inspection of the tandem mass spectra of the peptide ions assigned to these proteins. A list of all possible fragment ions (b-ions and y-ions) of each peptide was generated by performing in silico fragmentation of each peptides of interest using an online 'peptide fragmentation generator' tool (The University of Washington Proteomics Resource, 2011). The tandem mass spectrum of the identified peptide was then manually checked to confirm the correct assignment of the b-ions and y-ions within the mass accuracy of ± 0.5 Da (Da) (Suppl. Fig. S7). The MS1 mass spectra of these peptide precursor ion peaks were also inspected for background noise within an

isolation window of $\pm 1.5\,m/z$ around the precursor ion, as contaminant precursor ions could affect the iTRAQ quantitation.

Protein functional pathway analysis

We used DAVID (the Database for Annotation, Visualization and Integrated Discovery, v6.7, NCBI) to determine the molecular functions and subcellular localization of the identified 2847 total proteins. Functional and network analysis DE proteins was performed with Ingenuity Pathway Analysis (IPA) (Ingenuity® Systems). We used the 2847 total proteins as our reference dataset for the IPA analysis.

Appendix A. Supplementary materials

Supplementary data associated with this article can be found in the online version at http://dx.doi.org/10.1016/j.virol.2012.03.026.

References

Aebersold, R., Mann, M., 2003. Mass spectrometry-based proteomics. Nature 422 (6928), 198–207.

Barcova, M., Speth, C., Kacani, L., Uberall, F., Stoiber, H., Dierich, M.P., 1999. Involvement of adenylate cyclase and p70(S6)-kinase activation in IL-10 up-regulation in human monocytes by gp41 envelope protein of human immunodeficiency virus type 1. Pflugers Arch 437 (4), 538–546.

Benson, D.A., Karsch-Mizrachi, I., Lipman, D.J., Ostell, J., Sayers, E.W., 2011. GenBank. Nucleic Acids Res. 39(Database issue), D32–D37.

Bonaldi, T., Talamo, F., Scaffidi, P., Ferrera, D., Porto, A., Bachi, A., Rubartelli, A., Agresti, A., Bianchi, M.E., 2003. Monocytic cells hyperacetylate chromatin protein HMGB1 to redirect it towards secretion. EMBO J. 22 (20), 5551–5560.

Borchers, C., Tomer, K.B., 1999. Characterization of the noncovalent complex of human immunodeficiency virus glycoprotein 120 with its cellular receptor CD4 by matrix-assisted laser desorption/ionization mass spectrometry. Biochemistry 38 (36), 11734–11740.

Brass, A.L., Dykxhoorn, D.M., Benita, Y., Yan, N., Engelman, A., Xavier, R.J., Lieberman, J., Elledge, S.J., 2008. Identification of host proteins required for HIV infection through a functional genomic screen. Science 319 (5865), 921–926.

Bukrinsky, M.I., Haffar, O.K., 1998. HIV-1 nuclear import: matrix protein is back on center stage, this time together with Vpr. Mol. Med. 4 (3), 138–143.

Bushman, F.D., Malani, N., Fernandes, J., D'Orso, I., Cagney, G., Diamond, T.L., Zhou, H., Hazuda, D.J., Espeseth, A.S., Konig, R., Bandyopadhyay, S., Ideker, T., Goff, S.P., Krogan, N.J., Frankel, A.D., Young, J.A., Chanda, S.K., 2009. Host cell factors in HIV replication: meta-analysis of genome-wide studies. PLoS Pathog. 5 (5), e1000437.

Bustelo, X.R., 2002. Knocked out by Rho/Rac T-cell biology. Histol. Histopathol 17 (3), 871–875.

Cannon, J.L., Mody, P.D., Blaine, K.M., Chen, E.J., Nelson, A.D., Sayles, L.J., Moore, T.V., Clay, B.S., Dulin, N.O., Shilling, R.A., Burkhardt, J.K., Sperling, A.I., 2011. CD43 interaction with ezrin-radixin-moesin (ERM) proteins regulates T-cell trafficking and CD43 phosphorylation. Mol. Biol. Cell 22 (7), 954–963.

Chan, E.Y., Qian, W.J., Diamond, D.L., Liu, T., Gritsenko, M.A., Monroe, M.E., Camp 2nd, D.G., Smith, R.D., Katze, M.G., 2007. Quantitative analysis of human immunodeficiency virus type 1-infected CD4+ cell proteome: dysregulated cell cycle progression and nuclear transport coincide with robust virus production. J. Virol. 81 (14), 7571–7583.

Chan, E.Y., Sutton, J.N., Jacobs, J.M., Bondarenko, A., Smith, R.D., Katze, M.G., 2009. Dynamic host energetics and cytoskeletal proteomes in human immunodeficiency virus type 1-infected human primary CD4 cells: analysis by multiplexed label-free mass spectrometry. J. Virol. 83 (18), 9283–9295.

Chang, S.T., Sova, P., Peng, X., Weiss, J., Law, G.L., Palermo, R.E., Katze, M.G., 2011. Next-Generation Sequencing Reveals HIV-1-Mediated Suppression of T Cell Activation and RNA Processing and Regulation of Noncoding RNA Expression in a CD4+ T Cell Line. M. Bio. 2, 5.

Coiras, M., Camafeita, E., Urena, T., Lopez, J.A., Caballero, F., Fernandez, B., Lopez-Huertas, M.R., Perez-Olmeda, M., Alcami, J., 2006. Modifications in the human T cell proteome induced by intracellular HIV-1 Tat protein expression. Proteomics 6 (Suppl. 1), S63–S73.

Deutsch, E.W., Mendoza, L., Shteynberg, D., Farrah, T., Lam, H., Tasman, N., Sun, Z., Nilsson, E., Pratt, B., Prazen, B., Eng, J.K., Martin, D.B., Nesvizhskii, A.I., Aebersold, R., 2010. A guided tour of the Trans-Proteomic Pipeline. Proteomics 10 (6), 1150–1159.

Eisenberg, E., Levanon, E.Y., 2003. Human housekeeping genes are compact. Trends Genet. 19 (7), 362–365.

Fu, W., Sanders-Beer, B.E., Katz, K.S., Maglott, D.R., Pruitt, K.D., Ptak, R.G., 2009. Human immunodeficiency virus type 1, human protein interaction database at NCBI. Nucleic Acids Res. 37(Database issue), D417–D422.

Gruters, R.A., Terpstra, F.G., De Jong, R., Van Noesel, C.J., Van Lier, R.A., Miedema, F., 1990. Selective loss of T cell functions in different stages of HIV infection. Early loss of anti-CD3-induced T cell proliferation followed by decreased anti-CD3-induced cytotoxic T lymphocyte generation in AIDS-related complex and AIDS. Eur. J. Immunol. 20 (5), 1039–1044.

Hagner, P.R., Mazan-Mamczarz, K., Dai, B., Balzer, E.M., Corl, S., Martin, S.S., Zhao, X.F., Gartenhaus, R.B., 2011. Ribosomal protein S6 is highly expressed in non-Hodgkin lymphoma and associates with mRNA containing a 5' terminal oligopyrimidine tract. Oncogene 30 (13), 1531–1541.

Han, X., Aslanian, A., Yates 3rd, J.R., 2008. Mass spectrometry for proteomics. Curr. Opin. Chem. Biol. 12 (5), 483–490.

Ingenuity® Systems ⟨www.ingenuity.com⟩.

Jager, S., Cimermancic, P., Gulbahce, N., Johnson, J.R., McGovern, K.E., Clarke, S.C., Shales, M., Mercenne, G., Pache, L., Li, K., Hernandez, H., Jang, G.M., Roth, S.L., Akiva, E., Marlett, J., Stephens, M., D'Orso, I., Fernandes, J., Fahey, M., Mahon, C., O'Donoghue, A.J., Todorovic, A., Morris, J.H., Maltby, D.A., Alber, T., Cagney, G., Bushman, F.D., Young, J.A., Chanda, S.K., Sundquist, W.I., Kortemme, T., Hernandez, R.D., Craik, C.S., Burlingame, A., Sali, A., Frankel, A.D., Krogan, N.J., 2012. Global landscape of HIV-human protein complexes. Nature 481 (7381), 365–370.

Keller, A., Nesvizhskii, A.I., Kolker, E., Aebersold, R., 2002. Empirical statistical model to estimate the accuracy of peptide identifications made by MS/MS and database search. Anal. Chem. 74 (20), 5383–5392.

Kornfeld, H., Cruikshank, W.W., Pyle, S.W., Berman, J.S., Center, D.M., 1988. Lymphocyte activation by HIV-1 envelope glycoprotein. Nature 335 (6189), 445–448.

Levy, S., Avni, D., Hariharan, N., Perry, R.P., Meyuhas, O., 1991. Oligopyrimidine tract at the 5' end of mammalian ribosomal protein mRNAs is required for their translational control. Proc. Natl. Acad. Sci. USA 88 (8), 3319–3323.

MacPherson, J.I., Dickerson, J.E., Pinney, J.W., Robertson, D.L., 2010. Patterns of HIV-1 protein interaction identify perturbed host-cellular subsystems. PLoS Comput. Biol. 6 (7), e1000863.

Madrid, R., Janvier, K., Hitchin, D., Day, J., Coleman, S., Noviello, C., Bouchet, J., Benmerah, A., Guatelli, J., Benichou, S., 2005. Nef-induced alteration of the early/recycling endosomal compartment correlates with enhancement of HIV-1 infectivity. J. Biol. Chem. 280 (6), 5032–5044.

Malim, M.H., Emerman, M., 2008. HIV-1 accessory proteins—ensuring viral survival in a hostile environment. Cell Host Microbe 3 (6), 388–398.

Melendez, L.M., Colon, K., Rivera, L., Rodriguez-Franco, E., Toro-Nieves, D., 2011. Proteomic analysis of HIV-infected macrophages. J. Neuroimmune Pharmacol. 6 (1), 89–106.

Meng, L., Yasumoto, H., Tsai, R.Y., 2006. Multiple controls regulate nucleostemin partitioning between nucleolus and nucleoplasm. J. Cell Sci. 119 (Pt 24), 5124–5136.

Meyuhas, O., 2008. Physiological roles of ribosomal protein S6: one of its kind. Int. Rev. Cell Mol. Biol. 268, 1–37.

Miller, H.B., Robinson, T.J., Gordan, R., Hartemink, A.J., Garcia-Blanco, M.A., 2011. Identification of Tat-SF1 cellular targets by exon array analysis reveals dual roles in transcription and splicing. RNA 17 (4), 665–674.

Misse, D., Cerutti, M., Noraz, N., Jourdan, P., Favero, J., Devauchelle, G., Yssel, H., Taylor, N., Veas, F., 1999. A CD4-independent interaction of human immunodeficiency virus-1 gp120 with CXCR4 induces their cointernalization, cell signaling, and T-cell chemotaxis. Blood 93 (8), 2454–2462.

Montanaro, L., Trere, D., Derenzini, M., 2008. Nucleolus, ribosomes, and cancer. Am. J. Pathol. 173 (2), 301–310.

Nakada, S., Tai, I., Panier, S., Al-Hakim, A., Iemura, S., Juang, Y.C., O'Donnell, L., Kumakubo, A., Munro, M., Sicheri, F., Gingras, A.C., Natsume, T., Suda, T., Durocher, D., 2010. Non-canonical inhibition of DNA damage-dependent ubiquitination by OTUB1. Nature 466 (7309), 941–946.

Pedrioli, P.G., Raught, B., Zhang, X.D., Rogers, R., Aitchison, J., Matunis, M., Aebersold, R., 2006. Automated identification of SUMOylation sites using mass spectrometry and SUMmOn pattern recognition software. Nat. Methods 3 (7), 533–539.

Pinney, J.W., Dickerson, J.E., Fu, W., Sanders-Beer, B.E., Ptak, R.G., Robertson, D.L., 2009. HIV-host interactions: a map of viral perturbation of the host system. AIDS 23 (5), 549–554.

Ptak, R.G., Fu, W., Sanders-Beer, B.E., Dickerson, J.E., Pinney, J.W., Robertson, D.L., Rozanov, M.N., Katz, K.S., Maglott, D.R., Pruitt, K.D., Dieffenbach, C.W., 2008. Cataloguing the HIV type 1 human protein interaction network. AIDS Res. Hum. Retroviruses 24 (12), 1497–1502.

Ramaswamy, M., Dumont, C., Cruz, A.C., Muppidi, J.R., Gomez, T.S., Billadeau, D.D., Tybulewicz, V.L., Siegel, R.M., 2007. Cutting edge: Rac GTPases sensitize activated T cells to die via Fas. J. Immunol. 179 (10), 6384–6388.

Ringrose, J.H., Jeeninga, R.E., Berkhout, B., Speijer, D., 2008. Proteomic studies reveal coordinated changes in T-cell expression patterns upon infection with human immunodeficiency virus type 1. J. Virol. 82 (9), 4320–4330.

Ross, P.L., Huang, Y.N., Marchese, J.N., Williamson, B., Parker, K., Hattan, S., Khainovski, N., Pillai, S., Dey, S., Daniels, S., Purkayastha, S., Juhasz, P., Martin, S., Bartlet-Jones, M., He, F., Jacobson, A., Pappin, D.J., 2004. Multiplexed protein quantitation in Saccharomyces cerevisiae using amine-reactive isobaric tagging reagents. Mol. Cell Proteomics 3 (12), 1154–1169.

Speth, C., Prohaszka, Z., Mair, M., Stockl, G., Zhu, X., Jobstl, B., Fust, G., Dierich, M.P., 1999. A 60 kD heat-shock protein-like molecule interacts with the HIV transmembrane glycoprotein gp41. Mol. Immunol 36 (9), 619–628.

The University of Washington's Proteomic Resource Facility(UWPR) 〈http://proteomicsresource.washington.edu/MassSpecUtils.php〉 07.01.2011.

The University of Washington Environment Health and Safety 〈http://www.ehs.washington.edu/rbsbiosafe/index.shtm〉 06.2011.

The University of Washington Proteomics Resource 〈http://proteomicsresource.washington.edu/cgi-bin/fragment.cgi〉 09.02.2011.

UNAIDS 〈http://www.unaids.org/en/media/unaids/contentassets/dataimport/pub/report/2009/jc1700_epi_update_2009_en.pdf〉.

van't Wout, A.B., Lehrman, G.K., Mikheeva, S.A., O'Keeffe, G.C., Katze, M.G., Bumgarner, R.E., Geiss, G.K., Mullins, J.I., 2003. Cellular gene expression upon human immunodeficiency virus type 1 infection of CD4(+)-T-cell lines. J. Virol. 77 (2), 1392–1402.

Vodicka, M.A., Goh, W.C., Wu, L.I., Rogel, M.E., Bartz, S.R., Schweickart, V.L., Raport, C.J., Emerman, M., 1997. Indicator cell lines for detection of primary strains of human and simian immunodeficiency viruses. Virology 233 (1), 193–198.

Wang, H., Bloom, O., Zhang, M., Vishnubhakat, J.M., Ombrellino, M., Che, J., Frazier, A., Yang, H., Ivanova, S., Borovikova, L., Manogue, K.R., Faist, E., Abraham, E., Andersson, J., Andersson, U., Molina, P.E., Abumrad, N.N., Sama, A., Tracey, K.J., 1999. HMG-1 as a late mediator of endotoxin lethality in mice. Science 285 (5425), 248–251.

Wolf-Yadlin, A., Hautaniemi, S., Lauffenburger, D.A., White, F.M., 2007. Multiple reaction monitoring for robust quantitative proteomic analysis of cellular signaling networks. Proc. Natl. Acad. Sci. USA 104 (14), 5860–5865.

Wu, W.W., Wang, G., Baek, S.J., Shen, R.F., 2006. Comparative study of three proteomic quantitative methods, DIGE, cICAT, and iTRAQ, using 2D gel- or LC-MALDI TOF/TOF. J. Proteome Res. 5 (3), 651–658.

Zanin-Zhorov, A., Nussbaum, G., Franitza, S., Cohen, I.R., Lider, O., 2003. T cells respond to heat shock protein 60 via TLR2: activation of adhesion and inhibition of chemokine receptors. FASEB J. 17 (11), 1567–1569.

Zhou, Q., Sharp, P.A., 1996. Tat-SF1: cofactor for stimulation of transcriptional elongation by HIV-1 Tat. Science 274 (5287), 605–610.